



Gamma-Ray bursts: Energetics and Prompt Correlations

Amir Shahmoradi, Dept. of Physics, Institute for Fusion Studies, The University of Texas at Austin, TX 78712
Presented at: 7th Huntsville Gamma-Ray Burst Symposium, Nashville, TN, April 14-18, 2013

THE UNIVERSITY OF TEXAS AT AUSTIN



ABSTRACT

It is proposed that the luminosity function, the rest-frame spectral and temporal correlations and distributions of cosmological Long-duration (Type-II) Gamma-Ray Bursts (LGRBs) may be very well described as multivariate log-normal distribution. This result is based on careful selection, analysis and modeling of LGRBs' temporal and spectral variables in the largest catalog of Gamma-Ray Bursts available to date: 2130 BATSE GRBs, while taking into account the detection threshold and possible selection effects. Constraints on the joint rest-frame distribution of the isotropic peak luminosity (L_{bol}), total isotropic emission (E_{bol}), the time-integrated spectral peak energy (E_p) and duration (T_{90}) of LGRBs are derived. The presented analysis provides evidence for a relatively large fraction of LGRBs that have been missed by BATSE detector with E_{bol} extending down to $\sim 10^{49}$ [erg] and observed spectral peak energies (E_p) as low as ~ 5 [keV]. LGRBs with rest-frame duration $T_{90} < 1$ [s] or observer-frame duration $T_{90} < 2$ [s] appear to be rare events (<0.1% chance of occurrence). The model predicts a fairly strong but highly significant correlation ($\rho = 0.58 \pm 0.04$) between E_{bol} & E_p of LGRBs (the Amati relation). Also predicted are strong correlations of L_{bol} & E_p with T_{90} , and moderate correlation between L_{bol} & E_{bol} . The strength and significance of the correlations found encourage search for the underlying mechanisms; though undermine their capabilities as probes of Dark Energy's equation of state at high redshifts. The presented analysis favors -- but does not necessitate -- a cosmic rate for BATSE LGRBs tracing metallicity evolution consistent with a cutoff $Z/Z_{\odot} \sim 0.2 - 0.5$, assuming no luminosity-redshift evolution. A comparison with short-hard (type-I) class of GRBs will be given. It is shown that similar prompt γ -ray correlations are also present among spectral and temporal parameters of type-I GRBs, possibly indicating a unified prompt emission mechanism for both classes of long-soft and short-hard GRBs.

BACKGROUND

Despite significant progress over the past decade, difficulties in modeling the complex effects of detector threshold on the multivariate distribution of the prompt-emission properties and the lack of a sufficiently large sample of uniformly detected GRBs has led the GRB community to focus on individual spectral/temporal variables, most importantly, on the Luminosity Function (LF) of GRBs. A more accurate modeling of the LF, however, requires at least two variables incorporated in the LGRB world model: the bolometric peak flux (P_{bol}) and the observed peak energy (E_p). The parameter E_p is required, since most γ -ray detectors are photon counters, a quantity that depends on not only P_{bol} but also E_p of the burst. This leads to the requirement of using a bivariate distribution as the minimum acceptable LGRB world model to begin with, for the purpose of constraining the LF. For SGRBs, the joint trivariate distribution of P_{bol} , E_p and the observed duration (T_{90}) is the minimum acceptable model in order to correctly account for the detection threshold of most γ -ray detectors.

The goal of the presented analysis is,

- to provide a quantitative phenomenological classification method for GRBs based on the observed prompt γ -ray emission properties, independent of detector specifications and limitations.
- to derive a multivariate model that is capable of reproducing the luminosity function, energetics, duration distributions and the true underlying correlations among four main parameters of the prompt γ -ray emission in both classes of SGRBs & LGRBs: L_{bol} , E_{bol} , E_p , T_{90} , (Figure 1) while paying careful attention to selection effects and observational biases that might affect GRB data.
- to gauge the utility and strength of the claimed high-energy correlations among the spectral parameters of GRBs in cosmological studies, in particular, the study of Dark Energy's equation of state at high redshifts.

Toward this, the presented analysis is focused on the largest catalog of GRBs available to date: the BATSE catalog of 2130 GRBs.

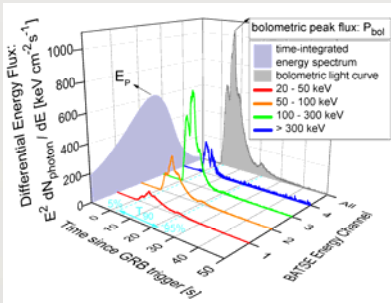


Figure 1. Example of GRB γ -ray light curve: BATSE trigger 1085, in different energy bands illustrating the definitions of the four GRB prompt emission variables used in this study: P_{bol} , S_{bol} , E_p , T_{90} . The violet and gray shaded areas both represent the bolometric fluence (S_{bol}).

SAMPLE SELECTION

The traditional definition of GRB classes is based on a sharp cutoff in the observed duration distribution (T_{90}) of GRBs, generally set at $T_{90} \sim 2-3$ [s]. Here, to ensure the least amount of bias in classification and correct analysis, BATSE GRBs are classified according to fuzzy C-means clustering algorithm, based on two GRB observables: T_{90} & E_p as shown in Figure 2 below (c.f., Shahmoradi 2013, Sec. 2.1 & Appendix A for details).

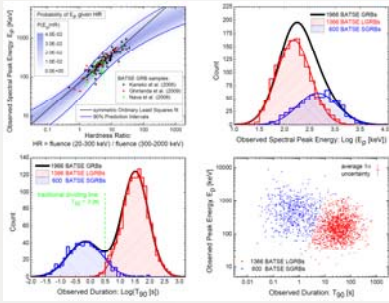


Figure 2. Top Left: Example graph depicting the strong correlation of E_p with Hardness Ratio (HR) of BATSE GRBs (c.f., Shahmoradi & Nemiroff 2010 for details). Top Right: Derived E_p distribution for 1966 BATSE GRBs based on $HR - E_p$ relation. Bottom Left: T_{90} distribution of 1966 BATSE GRBs. Bottom Right: The joint $T_{90} - E_p$ distribution of 1966 BATSE GRBs, classified according to fuzzy C-means clustering algorithm. The spectral peak energy (E_p) estimates of these events are taken from Shahmoradi & Nemiroff (2010), also publicly available for download at: <https://sites.google.com/site/amshportal/research/aca/in-the-news/lgrb-world-model>

MODEL CONSTRUCTION

Here, the multivariate log-normal distribution (LN) is proposed as the simplest natural candidate model, capable of describing data. The motivation behind this choice of model comes from the available observational data that closely resemble a joint multivariate log-normal distribution for the four most widely studied temporal and spectral parameters of GRBs in the observer frame: P_{bol} , S_{bol} , E_p , T_{90} , truncated by BATSE detection threshold -- since most GRBs originate from moderate redshifts $z \sim 1-3$, a fact known thanks to Swift satellite, the convolution of these observer-frame parameters with the redshift distribution results in negligible variation in the shape of the rest-frame joint distribution of the same GRB parameters.

The process of GRB observation is therefore considered as a non-homogeneous Poisson process whose mean rate parameter (i.e., the cosmic GRB differential rate), R_{cosmic} , is the product of the differential comoving GRB rate density (\dot{z}) with $p = 4D$ log-normal probability density function, LN , of four GRB variables: L_{bol} , E_{bol} , E_p , T_{90} , with location vector μ and the scale (i.e., covariance) matrix Σ ,

$$R_{\text{cosmic}} = \frac{dL_{\text{bol}} dE_{\text{bol}} dE_p dz}{L_{\text{bol}} E_{\text{bol}} E_p dz} \propto LN(L_{\text{bol}}, E_{\text{bol}}, E_p, T_{90}) | \mu, \Sigma \times \frac{dV}{dz}$$

where dV/dz is the comoving volume element per unit redshift. The observed rate of GRBs, R_{obs} , is the result of the convolution of the cosmic GRB rate, R_{cosmic} , with BATSE Large Area Detector threshold, $\eta(L_{\text{bol}}, E_{\text{bol}}, T_{90}, z)$,

$$R_{\text{obs}} = R_{\text{cosmic}} \times \eta(\text{detection}) | L_{\text{bol}}, E_{\text{bol}}, T_{90}, z$$

DETECTION THRESHOLD

The probability of detection for a GRB is modeled by the cumulative density function of log-normal distribution with mean and scale parameters μ_{thresh} & σ_{thresh} ,

$$\eta(\text{detection}) | \mu_{\text{thresh}}(T_{90}, z), \sigma_{\text{thresh}}(L_{\text{bol}}, E_{\text{bol}}, z) = \frac{1}{2} + \frac{1}{\sqrt{2}} \text{erf} \left(\frac{\log(P(L_{\text{bol}}, E_{\text{bol}}, z)) - \mu_{\text{thresh}}(T_{90}, z)}{\sqrt{2}\sigma_{\text{thresh}}} \right)$$

where $P(L_{\text{bol}}, E_{\text{bol}}, z)$ is the $1[s]$ peak photon flux in the BATSE nominal detection energy range: 50-300 [keV], and μ_{thresh} & σ_{thresh} are the detection threshold parameters to be determined by model fitting.

Based on the observation that almost all 1366 BATSE LGRBs have durations of $T_{90} > 1$ [s], the primary trigger timescale for BATSE LGRBs is assumed to be 1024 [ms]. This eliminates the relatively complex dependence of the detection probability (η) on the duration of the LGRB events. (c.f., Shahmoradi 2013: Appendix B for details of detection threshold modeling). For SGRBs, the situation is nontrivial and is discussed by Shahmoradi (2013, in preparation).

MODEL FITTING

The best-fit parameters are obtained by the method of maximum likelihood. This is done by maximizing the likelihood function of the model, given the observational data, using a variant of the Metropolis-Hastings Markov Chain Monte Carlo (MCMC) algorithm. The objective function to be maximized is,

$$\mathcal{L}(\text{Data} | \text{Model Parameters}) = A^N \exp \left(-A \int_{\text{Data}} R_{\text{obs}}(t) dt \right) \prod_{i=1}^N R_{\text{cosmic}}(L_{\text{bol}}, E_{\text{bol}}, E_p, T_{90} | \text{Model Parameters}) \mathcal{L}(\Omega_i | \mu, \Sigma, z_i)$$

To reduce the simulation runtime, all algorithms including MCMC are implemented in Fortran (2008 standard). An example of fitting results for 1366 BATSE LGRBs are given in Figure 3 and Figure 4 (c.f., Shahmoradi 2013: Sec. 2.4 for extensive goodness-of-fit tests and Appendix C for likelihood construction).

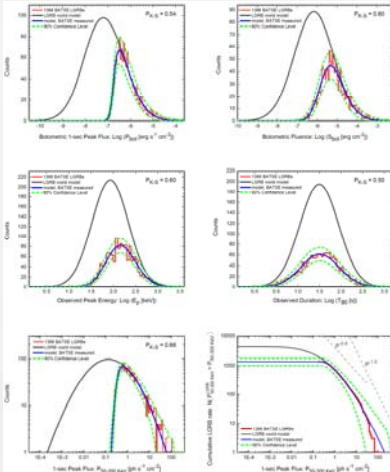


Figure 3. Top-Center: Marginal distribution predictions (solid blue lines) of the LGRB world model given BATSE detection efficiency, superposed on BATSE 1366 LGRB data (red histograms). The solid gray lines represent the model predictions for the entire LGRB population (detected and undetected), with no correction for BATSE sky exposure and the beaming factor. The 90% confidence intervals (dashed green lines) represent random Poisson fluctuations expected in the BATSE LGRB-detection process. Bottom: The differential (left panel) and cumulative (right panel) rate of LGRBs as a function of peak photon flux in the BATSE nominal detection energy range (50-300 keV). The Kolmogorov-Smirnov (K-S) test probabilities for the goodness-of-fit of the model predictions to BATSE data are reported at the top-right corner of each plot.

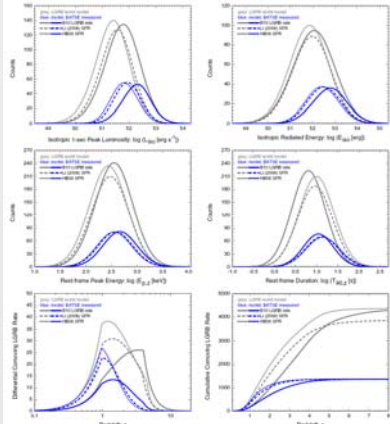


Figure 4. Top-Center: The marginal distribution predictions (blue lines) of the LGRB world model for BATSE LGRBs in the burst's rest frame. The gray lines represent model predictions for the entire LGRB population. Bottom: The three differential (left panel) and cumulative (right panel) redshift distributions of LGRBs considered in this study (c.f., Shahmoradi 2013: Figure 6 and references therein for redshift distributions).

CORRELATIONS

The prediction of the LGRB world model for the two most popular prompt γ -ray correlations of LGRBs are depicted in Figure 5.

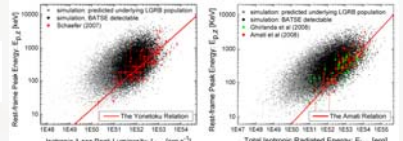


Figure 5. The Amati & Yonetoku relations, superposed on the LGRB world model predictions (c.f., Shahmoradi 2013: Sec. 3.4).

LGRBs VS. SGRBs

A similar population study of BATSE SGRBs (Figure 6) reveals correlations and joint distributions of parameters that are similar to LGRBs, despite the potentially different progenitors of the two GRB classes.

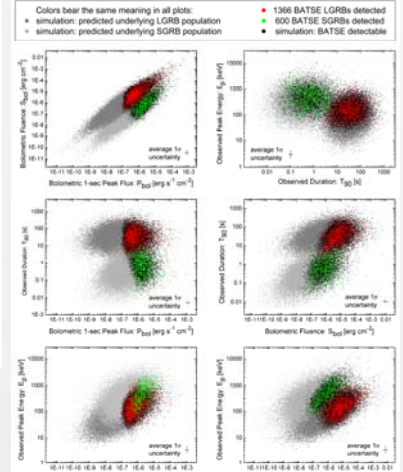


Figure 6. Plots of BATSE 1366 LGRBs and 600 SGRBs prompt emission data superposed on the bivariate distribution predictions of the world models for the two GRB classes (c.f., Shahmoradi 2013: Sec. 3).

COLLAPSR EVIDENCE?

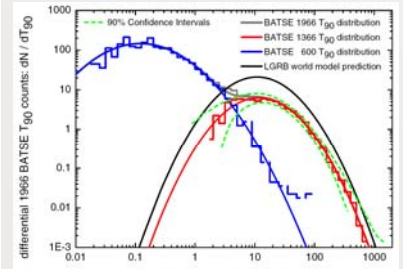


Figure 7. Recently Bromberg et al. (2012) proposed the apparent flatness in the duration distribution of BATSE LGRBs as the first direct evidence of the Collapsar model of LGRBs. The flat T_{90} distribution of LGRBs at short durations can be explained away in terms of the skewed nature of the log-normal distribution subject to sample incompleteness. Noticeably, similar flat distribution behavior is also observed for SGRBs.

REFERENCES

- Shahmoradi, A., 2013, The Astrophysical Journal, 766, 111.
- Shahmoradi, Amir and Nemiroff, Robert J., 2011, MNRAS, 411, 1843.
- Shahmoradi, Amir and Nemiroff, Robert J., 2010, MNRAS, 407, 2975.
- Shahmoradi, Amir and Nemiroff, Robert J., 2009, AIP Conference Proceedings, 1132, 1, 425-427.
- Nemiroff, Robert J. and Shahmoradi, Amir, 2009, AIP Conference Proceedings, 1133, 1, 323-327.

